Mechanically induced Helfrich-Hurault effect in a confined lamellar system with finite surface anchoring

Riccardo De Pascalis*

Dipartimento di Matematica e Fisica "E. De Giorgi", Università del Salento, Via per Arnesano, 73100, Lecce, Italy

(Received 14 May 2019; published 16 July 2019)

Soft lamellar phases confined between two parallel plates and subject to a dilatative strain can become unstable exhibiting periodic deformations patterns of the layers. By a variational energy approach, a critical threshold for the imposed *finite* strain is derived in the case of *weak anchoring* conditions. The potential, associated to the system, includes a two-terms energy which accounts for the bending of the layers and the dilatation of the bulk as well as an anchoring potential. Classical results for strong anchoring at the walls are recovered. It is shown that weak anchoring conditions can lead to a lower critical threshold of the field, similarly as happens for the instability induced by a magnetic or an electric field normal to the layers. Nevertheless, in the limit of weak anchoring, the model reveals that this instability does not occur. Analytical formulas are provided which certainly encourage further experimental investigations.

DOI: 10.1103/PhysRevE.100.012705

I. INTRODUCTION

Lamellar structures like cholesteric or smectic liquid crystals confined between two parallel plates and subject to external fields (electric, magnetic, as well as a mechanically deformation) can, under a certain critical threshold, become unstable and buckle into a new different configuration [1–4].

Cholesteric liquid crystal samples subject to a magnetic or electric field applied normally to its layers tend to reorient them along the normal, while the molecules anchored at the boundary walls do not allow the adjacent layers to freely rotate. In the early 1970s, Helfrich [5] and Hurault [6] first observed that this competition can lead to periodic undulations of the layers' orientation. This instability is nowadays known in literature as the *Helfrich-Hurault effect* [1]. Theoretical predictions for this instability and for an infinite sample can be found in Refs. [1,7], while theoretical results extended to finite samples of smectic-*A* liquid crystals, if subject to both a uniform pressure and a magnetic field, can be found in Ref. [8] and if subject to an electric field in Refs. [9,10]. Further theoretical results for the Helfrich-Hurault instability induced by a magnetic field but for smectic-*C* liquid crystals can be found in Refs. [11,12].

Ishikawa and Lavrentovich [13] observed the undulations of the layered systems of a cholesteric stripe phase with a macroscopic supramicron periodicity induced by an in-plane magnetic field normal to the layers. A few years later, Senyuk *et al.* [14] observed this instability for a confined cholesteric liquid crystal sample subject to an electrical field applied along the normal to the layers. Both studies [13,14] emphasize that a displacement of the layers immediately above the instability threshold is much larger than the values expected from the previous classical theories. They were able to describe their experimental data by including a finite anchoring potential to the wall, demonstrating [for the two-dimensional (2D) case in Ref. [13] and for the extended three-dimensional (3D) case in Ref. [14]] that the undulations depend from the molecules anchoring at the wall. Moreover they deduced, qualitatively and quantitatively, that the finite strong conditions can decrease the critical threshold applied field allowing larger displacements of the layers.

Undulations of the layers also can be caused by a dilatative mechanical applied deformation [15–20], where layers, in order to increase their effective thickness due to the dilatation, tend to tilt and to balance the stretch imposed to the sample, which tends to separate the boundary walls. All these studies are, however, confined to the case of strong anchoring conditions. In particular, Refs. [18,19] explored the case of nonlinear undulations where the instability shows a transition from sinusoidal to a chevron structure. Napoli and Nobili [20] extended the classical results valid for infinitesimal imposed strain [see Eq. (40)] to the most general case valid for an imposed finite dilatative strain [see Eq. $(39)_1$], capable therefore of covering cases where the specimen thickness d can be comparable to the characteristic length λ. Analogous observed instabilities are reported in Refs. [21,22]. The former refers to active cholesteric liquid crystals where buckling can be induced by both extensile or contractile applied stresses, while the latter concerns freely floating smectic liquid crystalline films [22] where spontaneous wrinkling can appear in order to compensate lateral compressions.

Here the Helfrich-Hurault effect is analyzed for an infinite *smectic-A liquid crystals* sample which exhibits homeotropic alignments of the layers, and it is subjected to a dilatative finite applied strain along the normal to the layers when molecules are weakly anchored at the walls. By a variational energy approach, a critical strain γ_c at which buckling can occur is investigated for the symmetric anchoring case. The energy associated to the system includes a classical two-terms energy, with one term associated to the bending of the layers and the other associated to the dilatation of the bulk [see Eq. (11)],

*riccardo.depascalis@unisalento.it

as well as a Rapini and Papoular-type anchoring potential [23] at the walls [see Eq. (16)]. Classical results for strong anchoring conditions are recovered [1,15,16], noticing that the derived model is valid to describe both the infinitesimal and the finite applied strain case (see Ref. [20] for further details). Noteworthy, for example, are the experimental findings on the cholesteric fingerprint texture with a macroscopic ≈ 10 mm periodicity; this profile deviates from the classic pattern predicted by the linear elastic theory but fits well with the nonlinear theory of dislocations [24,25].

Furthermore, in analogy with a sample subject to a magnetic [13] or electric field [14] normal to the layers, respectively, here we show also that a similar result is still valid, i.e., finite anchoring conditions lead to the lower critical threshold field. Nevertheless, the equations derived from this model reveal that, in the limit of weak anchoring, the type of instability considered here does not occur. An analytical expression for the anchoring strength bound in terms of $\eta = \lambda/d$, beyond which the instability is not predicted from this model, is provided. Worth noting that this feature is also exhibited from the critical field derived in Ref. [13] for the sample subject to an external magnetic field normal to the layers. In order to explore the limit case of weak anchoring conditions further experimental investigations are therefore encouraged. Remarkably, observations have been made of cholesteric liquid crystal samples with a short pitch, which can behave as a layered smectic-*A* liquid crystal, and for which under an applied electric field sufficiently larger than the anchoring energy, the nonlinear undulations can be transformed to a system of defects [26,27].

The paper is organized as follows: Sec. II introduces the geometry of the sample and the applied deformation field as well as the assumptions on the energy associated to it. In Sec. III, in order to compute the critical threshold, the Euler-Lagrange equation with boundary conditions at the walls are derived by a variational approach. These equations are then specialized to the symmetric anchoring in Sec. IV, where analytical formulas for the whole critical field are derived. Importantly, it is shown that the limit for strong anchoring conditions is recovered, while the instability does not occur for very weak anchoring. In this last section, we provide this analytical cutoff critical bound as well as a general discussion of the obtained results.

II. THE MODEL

A. Geometric preliminaries

Smectic-*A* liquid crystals can be described by isosurfaces φ_k (k labels the layer) defined by

$$\varphi(\mathbf{x}, k) = 0, \tag{1}$$

where $\mathbf{x}$ denotes the current vector position of a point on φ_k. In particular, in the undeformed state such surfaces are parallel planes described by the relationship

$$\varphi_0(\mathbf{X}, k) = \mathbf{N} \cdot \mathbf{X} - k\ell_0, \tag{2}$$

where $\mathbf{X} = X\mathbf{E}_1 + Z\mathbf{E}_3$ is a position vector of a point written in its undeformed coordinates, $\mathbf{N}$ denotes the unit normal vector $\mathbf{N} \equiv \mathbf{E}_3$, while ℓ_0 represents the distance between the considered plane and the reference plane $Z = 0$, where

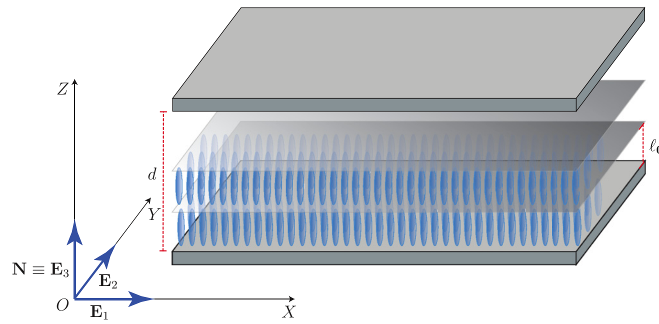

FIG. 1. A sample of a smectic-*A* liquid crystal in the undeformed configuration (no scale is implied).

(X, Y, Z) is a Cartesian reference frame (see Fig. 1 for a schematic representation of the sample in the undeformed configuration). The operator "$\cdot$" denotes the inner product.

Let us consider the invertible transformation $\mathbf{x} = \chi(\mathbf{X})$, which maps the undeformed configuration into the distorted one described, in a Cartesian coordinate system, by (x, y, z). By using its inverse $\mathbf{X} = \chi^{-1}(\mathbf{x})$, Eq. (2) can be rewritten as

$$\varphi(\mathbf{x}, k) = \mathbf{N} \cdot \chi^{-1}(\mathbf{x}) - k\ell_0. \tag{3}$$

Let us denote by $\mathbf{F}$ the deformation gradient of the transformation χ, which, in component form, is given by $F_{ij} = (\text{Grad}\mathbf{x})_{ij} = \partial x_i/\partial X_j$, $(i, j = 1, 2, 3)$. By taking the spatial gradient of Eq. (3) with respect to $\mathbf{x}$ coordinates and by application of the chain rule,

$$\nabla\varphi = \frac{\partial\varphi}{\partial\mathbf{x}} = \frac{\partial\varphi_0}{\partial\mathbf{X}}\frac{\partial\mathbf{X}}{\partial\mathbf{x}} = \mathbf{F}^{-\mathrm{T}}\frac{\partial\varphi_0}{\partial\mathbf{X}}, \tag{4}$$

where the superscript "$-$T" denotes the transpose of the inverse, so that

$$\nabla\varphi = \mathbf{F}^{-\mathrm{T}}\mathbf{E}_3. \tag{5}$$

A cell of material, which is in the homeotropic alignment, between two parallel planes $Z = 0$ and $Z = d$ is subjected to the following deformation:

$$\mathbf{x} = \mathbf{X} + U(X, Z)\mathbf{E}_3, \tag{6}$$

which, in the XZ plane, gives

$$\mathbf{F} = \begin{pmatrix} 1 & 0 & 0 \\ 0 & 1 & 0 \\ \partial_X U & 0 & 1 + \partial_Z U \end{pmatrix}, \quad \mathbf{F}^{-\mathrm{T}} = \begin{pmatrix} 1 & 0 & \frac{-\partial_X U}{1+\partial_Z U} \\ 0 & 1 & 0 \\ 0 & 0 & \frac{1}{1+\partial_Z U} \end{pmatrix}, \tag{7}$$

where ∂_X and ∂_Y denote the partial derivatives with respect to X and Y, respectively. From (5) and $(7)_2$ it follows that

$$|\nabla\varphi|^2 = \frac{1 + (\partial_X U)^2}{(1 + \partial_Z U)^2}. \tag{8}$$

Let consider the displacement U as a small perturbation superposed to a finite homogeneous displacement,

$$U(X, Z) = \gamma Z + \epsilon u(X, Z), \tag{9}$$

where $\gamma > 0$ is a strain along the Z direction and ϵ represents a small perturbative dimensionless positive parameter

$$\epsilon = \sqrt{\frac{\gamma}{\gamma_c} - 1}, \tag{10}$$

where γ_c is the critical strain at which buckling occurs. Note that for $\epsilon = 0$ the ℓ_0 distance changes to a current distance ℓ given by $\ell = (1+\gamma)\ell_0$.

B. Distortion energy density

When a deformation field is imposed, the layers can undergo a static distortion with respect to their natural configuration. The free energy related to this distortion is the elastic energy density [28]

$$f_e = \frac{K}{2}(\text{div } \mathbf{n})^2 + \frac{B}{2}\left(\frac{1}{|\nabla\varphi|} - 1\right)^2, \tag{11}$$

where K and B are two positive constants called the *bending stiffness* and the *compression modulus*, respectively, and where $\mathbf{n}$ is the unit normal vector in the current configuration,

$$\mathbf{n} = \frac{\nabla\varphi}{|\nabla\varphi|}. \tag{12}$$

The first term of (11) penalizes the layer bending, since $\frac{1}{2}\text{div } \mathbf{n}$ represents the mean curvature of the layer surface. The second term represents the energy related to the dilation or compression of the layers thickness.

By application of the chain rule, we obtain

$$\text{div}\mathbf{n} = \text{Grad}\mathbf{n} \cdot \mathbf{F}^{-\text{T}} = \text{Tr}(\mathbf{F}^{-1}\text{Grad}\mathbf{n}) = -\epsilon\partial_{XX}u + O(\epsilon^2), \tag{13}$$

while

$$\frac{1}{|\nabla\varphi|} - 1 = \gamma + \epsilon\partial_Z u - \frac{\epsilon^2}{2}(1+\gamma)(\partial_X u)^2, \tag{14}$$

so that, up to the second order in ϵ, the elastic energy density (11) can be written as

$$f_e = \frac{1}{2}K(\partial_{XX}u)^2\epsilon^2 + \frac{B}{2}\{\gamma^2 + 2\gamma\epsilon\partial_Z u + \epsilon^2[(\partial_Z u)^2 - \gamma(\gamma+1)(\partial_X u)^2]\} + O(\epsilon^3). \tag{15}$$

C. Anchoring potential

According to the Rapini and Papoular formula [23], we assume that, at the walls, $\mathbf{n}$ prefers to align along the $\mathbf{E}_3$ direction. Consequently, the anchoring energy takes the form

$$f_a = \tfrac{1}{2}\left[w_-(\mathbf{n}\cdot\mathbf{E}_1)^2_{Z=0} + w_+(\mathbf{n}\cdot\mathbf{E}_1)^2_{Z=d}\right], \tag{16}$$

where $w_\pm$ are two positive constants, and $\mathbf{n}$ is the unit normal vector (12) in the deformed configuration, given by

$$\mathbf{n} = \frac{1}{\sqrt{1+\epsilon^2 u_X^2}}(-\epsilon u_X\mathbf{E}_1 + \mathbf{E}_3). \tag{17}$$

D. Nondimensionalization

The quantity $\lambda = \sqrt{K/B}$ defines a *characteristic length* of the material which is of the order of the layer thickness, while K/w, named the *extrapolation length*, is the measure for the relevance of the competing elastic distortion versus the anchoring induced order. Let define the nondimensional parameters

$$\xi = \frac{X}{d}, \quad \zeta = \frac{Z}{d}, \quad \upsilon = \frac{u}{d}, \quad \eta = \frac{\lambda}{d}, \quad \beta_\pm = \frac{d}{K}w_\pm, \tag{18}$$

which allow us to rewrite the energies densities (11) and (16) in a dimensionless form,

$$\begin{aligned}\phi_e &= f_e\frac{d^2}{K} \\ &= \frac{1}{2}(\upsilon_{\xi\xi})^2\epsilon^2 + \frac{1}{2\eta^2}\{\gamma^2 + 2\gamma\epsilon\upsilon_\zeta \\ &\quad + \epsilon^2[\upsilon_\zeta^2 - \gamma(\gamma+1)\upsilon_\xi^2]\} + O(\epsilon^3)\end{aligned} \tag{19}$$

and

$$\phi_a = f_a\frac{d}{K} = \frac{1}{2}\left[\beta_-\upsilon_\xi^2(\xi,0) + \beta_+\upsilon_\xi^2(\xi,1)\right]\epsilon^2 + O(\epsilon^4), \tag{20}$$

respectively. The quantities β_- and β_+ given in Eq. (18) measure the strength of the anchoring at the wall $\zeta = 0$ and $\zeta = 1$, respectively (see Ref. [1] for further details). Note that the strong planar anchoring conditions, where layers are clamped at the walls, are recovered in the limit $\beta_\pm \to \infty$. On the other hand, the conditions $\beta_\pm = 0$ expresses free anchoring conditions, and, in this case, the layers are *simply supported* at the walls.

III. CRITICAL THRESHOLD

We assume that the perturbative displacement field is separable in ζ and ξ by an amplitude unknown ζ-dependent function and a periodic cosine ξ-dependent function [2,20],

$$\upsilon(\xi,\zeta) = a(\zeta)\cos(q_\xi\xi), \tag{21}$$

with q_ξ representing a dimensionless wave number along the x direction. By integrating the total energy density $\phi_e + \phi_a$ with respect to ξ and averaging it over the period $T = 2\pi/q_\xi$, and then by integrating it with respect to the ζ variable in [0,1], we obtain the total potential of the system

$$\Phi = \frac{\gamma^2}{2\eta^2} + \frac{\epsilon^2}{4\eta^2}\int_0^1 \Psi(a,a')\,d\zeta + \frac{\epsilon^2}{4}q_\xi^2[\beta_- a^2(\zeta)_{|\zeta=0} + \beta_+ a^2(\zeta)_{|\zeta=1}] + O(\epsilon^3), \tag{22}$$

where $\Psi(a,a') = \Lambda a^2 + a'^2$ with the prime denoting the differentiation of a function with respect to its argument and

$$\Lambda = q_\xi^2\left[q_\xi^2\eta^2 - \gamma_c(\gamma_c+1)\right]. \tag{23}$$

Equilibrium configurations are stationary points of the free energy functional Φ. By considering a certain test function α, we impose

$$\Phi'(a)(\alpha) = \frac{\text{d}}{\text{d}t}\Phi(a+t\alpha)_{|t=0} = 0, \tag{24}$$

and at second order in ϵ, after carrying some straightforward algebra and from the arbitrariness of the function α, we deduce the Euler-Lagrange equation for a:

$$a'' - \Lambda a = 0, \tag{25}$$

which must also satisfy the following boundaries conditions (BCs):

$$a' - \beta_- \eta^2 q_\xi^2 a = 0, \quad \text{at } \zeta = 0, \tag{26}$$

$$a' + \beta_+ \eta^2 q_\xi^2 a = 0, \quad \text{at } \zeta = 1. \tag{27}$$

Note that γ positive ensures Λ negative. Thus, the most general solution of Eq. (25) can be written as combination of sine and cosine functions as

$$a(\zeta) = C_1 \cos(q_\zeta \zeta) + C_2 \sin(q_\zeta \zeta), \tag{28}$$

where q_ζ denotes a dimensionless wave number along the z direction and where C_1, C_2 are two integration constants. BCs (26) and (27) allow us to obtain one of these constants as well as the relation imposed to q_ζ and q_ξ:

$$C_1 = \frac{C_2 q_\zeta}{\beta_- \eta^2 q_\xi^2}, \quad f(q_\zeta, q_\xi) = 0, \tag{29}$$

where

$$f(q_\zeta, q_\xi) = \left(\beta_- \beta_+ \eta^4 q_\xi^4 - q_\zeta^2\right) \sin q_\zeta + (\beta_- + \beta_+)\eta^2 q_\xi^2 q_\zeta \cos q_\zeta. \tag{30}$$

IV. SYMMETRIC ANCHORING: RESULTS AND DISCUSSION

In the symmetric anchoring case $\beta_- = \beta_+ = \beta$, in order to take into account the imposed symmetry at the walls as well as to cover results for strong anchoring conditions [13,20], we can further assume a to be of the form

$$a(\zeta) = A \cos\left[q_\zeta\left(\tfrac{1}{2} - \zeta\right)\right], \tag{31}$$

where the amplitude A is a constant to be determined. Note that BCs (26) and (27) reduce now to one independent relation

$$q_\xi^2 = \frac{q_\zeta}{\beta \eta^2} \tan(q_\zeta/2), \tag{32}$$

which has to be satisfied with the constraint given by imposing a in Eq. (31) being a solution of (25):

$$q_\zeta^2 = -\Lambda. \tag{33}$$

By the assumption of the solution made in Eqs. (21) and (31), respectively, the minimization of the total energy (22) with respect to q_ξ allows us to determine the critical wave number

$$q_\xi^2 = \frac{\gamma_c(\gamma_c + 1)}{2\eta^2} - \beta q_\zeta \frac{1 + \cos q_\zeta}{q_\zeta + \sin q_\zeta}, \tag{34}$$

which, combined with (32) and (33), gives rise a nonlinear equation for the wave number q_ζ:

$$\tan^2\left(\frac{q_\zeta}{2}\right) + \beta^2 \eta^2 \frac{\sin q_\zeta - q_\zeta}{\sin q_\zeta + q_\zeta} = 0. \tag{35}$$

In terms of the existence of solutions for q_ζ, Eq. (35) exhibits a different behavior in the limit of strong anchoring from that of finite weak anchoring. While it guarantees solutions q_ζ for any large value of the strength parameter β, on the other hand (35) reveals a lower β cutoff bound, which clearly depends on η, and beyond which q_ζ solutions do not exist. Indeed, by expanding β in powers of q_ζ up to order two, it must hold

$$\beta = \frac{\sqrt{3}}{\eta} + \frac{q_\zeta^2}{5\sqrt{3}\eta} + O\left(q_\zeta^4\right), \tag{36}$$

which provides the lower expected β (at a fixed η) for the occurrence of the instability as $q_\zeta \to 0$. Note that Eq. (35) is the equivalent of Eq. (5) in Ref. [13] when a sample of cholesteric is subjected to a magnetic field normal to the layers.

By replacing the β expression from (35) into (32) and (33) and after straightforward algebra, we can derive the expression for γ_c and q_ξ in terms of the computed critical q_ζ and the parameter η:

$$\gamma_c = \frac{1}{2}\left(-1 + \sqrt{1 + 8\eta q_\zeta^2 \sqrt{\frac{1}{q_\zeta^2 - \sin^2 q_\zeta}}}\right),$$

$$q_\xi^2 = \frac{q_\zeta}{\eta}\sqrt{\frac{q_\zeta - \sin q_\zeta}{q_\zeta + \sin q_\zeta}}, \tag{37}$$

respectively. For $q_\zeta \approx 0$ they become

$$\gamma_c = \frac{1}{2}\left(-1 + \sqrt{1 + 8\sqrt{3}\eta}\right) + \frac{2\eta q_\zeta^2}{5\sqrt{3 + 24\sqrt{3}\eta}} + O\left(q_\zeta^4\right),$$

$$q_\xi^2 = \frac{q_\zeta^2}{2\sqrt{3}\eta} + O\left(q_\zeta^4\right), \tag{38}$$

respectively, which allows us to find easily their bounds values as $q_\zeta \to 0$.

According to the experimental setup carried in Ref. [13], let us consider $\lambda = 2.9\,\mu$m and $d = 1.7$ mm, which set $\eta = \eta_{\text{IL}} \approx 1.7 \times 10^{-3}$. Figure 2 shows the predictions for the critical wave numbers q_ζ and q_ξ, against the scaled strength anchoring $\bar{\beta} = 10^{-3}\beta$ and predicted by (35) and $(37)_2$, respectively. Note, from Fig. 2(a), that the classical limit $q_\zeta \to \pi$ of strong anchoring conditions is recovered [13,15,20]. Indeed, as $\beta \to \infty$ the relationship (32) imposes $q_\zeta \to k\pi$ (with k a nonzero integer number), and this nontrivial critical minimum threshold is obviously attained for $k = 1$, i.e., at $q_\zeta = \pi$. Consequently, in this limit, from (37) the critical strain γ_c and critical wave number q_ξ reduce to

$$\gamma_c = -\frac{1}{2} + \frac{1}{2}\sqrt{1 + 8\pi\eta}, \quad q_\xi = \sqrt{\frac{\pi}{\eta}}, \tag{39}$$

in agreement with Ref. [20], where it is remarked that, for $\eta \ll 1$, $(39)_1$ reduces to a classical linear result [1,15,16]:

$$\gamma_0 = 2\pi\eta. \tag{40}$$

Instead, for very low β, curves in Fig. 2(a) follow the law (36) and those in Fig. 2(b) the law $(37)_2$.

Figure 3 shows several predictions of γ_c/η versus $\bar{\beta}$, for η in a range $[\eta_{\text{IL}}, 60\eta_{\text{IL}}]$ where $\eta = 60\eta_{\text{IL}} \approx 0.1$. First, note that all curves are monotonic in β, confirming here the analogous result given in Refs. [13,14], i.e., finite anchoring at the walls favors (compared to the case of strong anchoring) the instability. Nevertheless, it is worth noting that all curves arise from a lower cutoff bound [represented in the graph by a

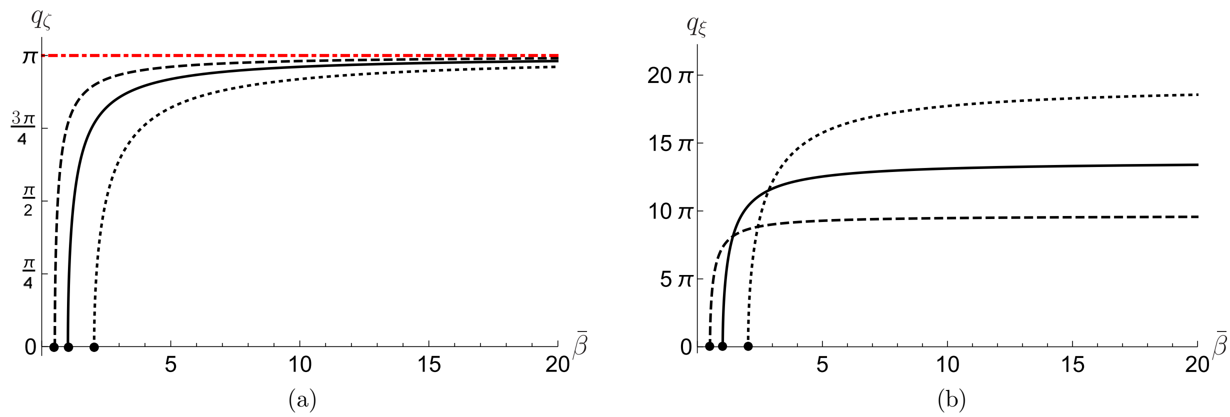

FIG. 2. The critical wave numbers when $\eta = \eta_{\rm IL}$ (solid line), $\eta = 1/2\eta_{\rm IL}$ (dotted line), and $\eta = 2\eta_{\rm IL}$ (dashed line) against $\bar{\beta} = 10^{-3}\beta$ and predicted by (35) (a) and $(37)_2$ (b), respectively.

red dashed curve obtained in the continuous limit $q_\zeta \to 0$ according to (36) and $(38)_1$]. Thus, the model suggests that very weak anchoring of molecules at the boundary walls might not be sufficient for the system to compensate for the effect instead observed for stronger anchoring conditions and instability is not favored. Finally, as $\bar{\beta} \to \infty$, all the curves tend asymptotically to a different limit γ_c/η according to (39) in disagreement with the classical limit $\gamma_0/\eta \to 2\pi$ given by using (40).

The derived model accounts for an instability of the Helfrich-Hurault type induced from an incremental deformation superposed to a finite homogeneous dilatation of the cell along the normal to the layers. The obtained results are therefore valid to predict the instabilities occurring in the linear case $\eta \ll 1$ as well as to recover the case for larger η. In the particular case when strong anchoring at the walls is applied, Napoli *et al.* [20] showed (see their Fig. 2) the discrepancy between γ_0 and γ_c versus η, which becomes significant for cell thickness d comparable to the characteristic length λ. In fact, considering a 1-stearoyl-2oleoyl-3-sn-phospatidylcholine sample of thickness $d = 40$ Å and $\lambda \approx 4.47$ Å ([29–31]), which implies $\eta \approx 0.09$, they showed a 29% difference between the classical γ_0 and γ_c. According

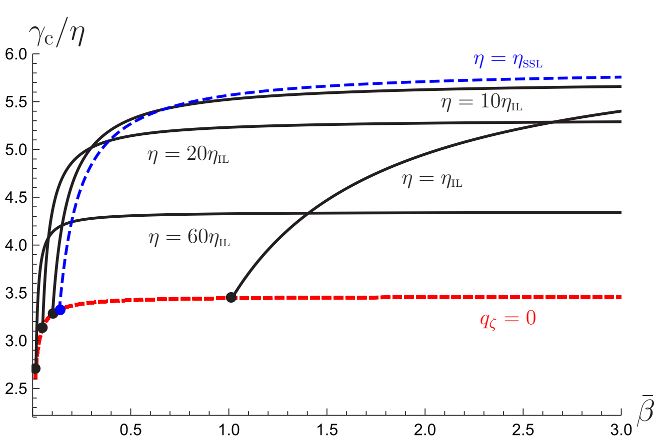

FIG. 3. Predictions of γ_c scaled by η against $\bar{\beta} = 10^{-3}\beta$ for several values of η. The red dashed curve shows the lower cutoff bound for $q_\zeta = 0$.

to the parameters set deduced in Ref. [14] for a cholesteric liquid crystal confined between two parallel planes subject to an electric field applied along the normal to the layers, $B \approx 10\,\mathrm{J/m^3}$, $K = 5.8$ pN, and $d \approx 60\,\mu$m, which imply $\eta = \eta_{\rm SSL} \approx 0.013$. In this latter case and for strong anchoring conditions the differences between γ_c and γ_0 would be of the 8%. Although it is still reasonable small, this disagreement there would be more consistent for weaker anchoring conditions whereas it has been observed larger layer displacements (see Ref. [14]). The present model would also therefore predict more accurately those most general cases.

To conclude the analysis, at the critical threshold, the incremental deformation field can therefore be written as

$$\upsilon(\xi,\zeta) = A\cos\left[q_\zeta\left(\tfrac{1}{2}-\zeta\right)\right]\cos(q_\xi\xi), \tag{41}$$

with q_ζ given as a solution of (35) and q_ξ given by $(37)_2$ and where the amplitude A is still an unknown of the problem. Following the proposed scheme in Refs. [13,32], in order to compute A, we impose to the total energy (22) a perturbed strain $\gamma = \gamma_c(1+\epsilon^2)$, and we retain it up to its fourth-order term in ϵ:

$$\begin{aligned}\Phi = {}& \frac{\gamma_c^2}{2\eta^2} + \frac{\epsilon^2}{4\eta^2}\left\{\int_0^1 (a'^2 + \Lambda a^2)\,d\zeta + 4\gamma_c^2\right.\\ &\left. + \eta^2\beta q_\xi^2[a^2(0)+a^2(1)]\right\}\\ &+ \frac{\epsilon^4}{64\eta^2}\left(\int_0^1 q_\xi^2 a^2\{3q_\xi^2 a^2[\gamma_c(4\gamma_c+5) - 4\eta^2 q_\xi^2 + 1]\right.\\ &- 4[a'^2 + 4\gamma_c(2\gamma_c+1)]\}\,d\zeta + \frac{\gamma_c^2}{2}\\ &\left. - 12\eta^2 q_\xi^4\beta[a^4(0)+a^4(1)]\right) + O(\epsilon^5).\end{aligned} \tag{42}$$

The minimization of the fourth-order term in ϵ of (42) with respect to A allows us to find the unknown amplitude $A \neq 0$, which is a solution of the following second-order equation:

$$\mathcal{C}A^2 + \mathcal{D} = 0 \tag{43}$$

with

$$\mathcal{C} = \frac{1}{64}\{2q_\zeta[-4q_\zeta^2 + 2q_\zeta \sin(2q_\zeta) + 9\Gamma q_\xi^2] + 3\Gamma q_\xi^2[8\sin q_\zeta + \sin(2q_\zeta)]\} - 6\beta\left[\eta^2 q_\zeta q_\xi^2 \cos^4\left(\frac{q_\zeta}{2}\right)\right] \tag{44}$$

and

$$\mathcal{D} = -\gamma_c(1+2\gamma_c)(q_\zeta + \sin q_\zeta), \tag{45}$$

where $\Gamma = 1 + \gamma_c(5+4\gamma_c) - 4\eta^2 q_\xi^2$. Finally, in the limit of strong anchoring $\beta \to \infty$ the results given in Ref. [20],

$$A = \pm 4\sqrt{\frac{2}{\pi}}\sqrt{\frac{\eta(1+8\pi\eta - \sqrt{1+8\pi\eta})}{9+64\pi\eta+9\sqrt{1+8\pi\eta}}}, \tag{46}$$

are also recovered, which show that for $\eta \ll 1$, the amplitude A can be approximated by

$$A = \pm\frac{8}{3}\eta \mp \frac{128\pi}{27}\eta^2 \pm \frac{1360\pi^2}{81}\eta^3 + O(\eta^4). \tag{47}$$

ACKNOWLEDGMENT

The author is grateful to Gaetano Napoli for fruitful discussions on this topic.

[1] P. de Gennes and J. Prost, *The Physics of Liquid Crystals*, 2nd ed. (Clarendon Press, Oxford, 1993).
[2] I. W. Stewart, *The Static and Dynamic Continuum Theory of Liquid Crystals: A Mathematical Introduction*, Liquid Crystals Book Series (Taylor and Francis, London, 2004).
[3] P. Oswald and P. Pieranski, *Smectic and Columnar Liquid Crystals: Concepts and Physical Properties Illustrated by Experiments* (CRC Press, Boca Raton, FL, 2005).
[4] A. Jákli, O. D. Lavrentovich, and J. V. Selinger, Rev. Mod. Phys. **90**, 045004 (2018).
[5] W. Helfrich, Appl. Phys. Lett. **17**, 531 (1970).
[6] J. P. Hurault, J. Chem. Phys. **59**, 2068 (1973).
[7] S. Chandrasekhar, *Liquid Crystals*, 2nd ed. (Cambridge University Press, Cambridge, 1992).
[8] I. W. Stewart, Phys. Rev. E **58**, 5926 (1998).
[9] G. Bevilacqua and G. Napoli, Phys. Rev. E **72**, 041708 (2005).
[10] G. Bevilacqua and G. Napoli, Mol. Cryst. Liq. Cryst. **436**, 127 (2005).
[11] I. W. Stewart, Liq. Cryst. **30**, 909 (2003).
[12] A. J. Walker and I. W. Stewart, J. Phys. A **40**, 11849 (2007).
[13] T. Ishikawa and O. D. Lavrentovich, Phys. Rev. E **63**, 030501(R) (2001).
[14] B. I. Senyuk, I. I. Smalyukh, and O. D. Lavrentovich, Phys. Rev. E **74**, 011712 (2006).
[15] N. A. Clark and R. B. Meyer, Appl. Phys. Lett. **22**, 493 (1973).
[16] M. Delaye, R. Ribotta, and G. Durand, Phys. Lett. A **44**, 139 (1973).
[17] R. Ribotta and G. Durand, J. Phys. **38**, 179 (1977).
[18] S. J. Singer, Phys. Rev. E **48**, 2796 (1993).
[19] P. Oswald, J.-C. Géminard, L. Lejvcek, and L. Sallen, J. Phys. II **6**, 281 (1996).
[20] G. Napoli and A. Nobili, Phys. Rev. E **80**, 031710 (2009).
[21] C. A. Whitfield, T. C. Adhyapak, A. Tiribocchi, G. P. Alexander, D. Marenduzzo, and S. Ramaswamy, Eur. Phys. J. E **40**, 50 (2017).
[22] K. Harth, T. Trittel, K. May, and R. Stannarius, Soft Matter (2019), doi:10.1039/C9SM01181A.
[23] A. Rapini and M. Papoular., J. Phys. Colloque **30**, C4-54 (1969).
[24] T. Ishikawa and O. D. Lavrentovich, Phys. Rev. E **60**, R5037 (1999).
[25] E. A. Brener and V. I. Marchenko, Phys. Rev. E **59**, R4752 (1999).
[26] L. Lejček, V. Novotná, and M. Glogarová, Liq. Cryst. (2018), doi:10.1080/02678292.2018.1550689.
[27] V. Novotná, V. Hamplová, M. Glogarová, L. Lejček, and E. Gorecka, Liq. Cryst. **45**, 634 (2018).
[28] G. Napoli, IMA J. Appl. Math. **71**, 34 (2006).
[29] R. Fettiplace, D. M. Andrews, and D. A. Haydon, J. Membr. Biol. **5**, 277 (1971).
[30] S. Hladky and D. Gruen, Biophys. J. **38**, 251 (1982).
[31] E. Evans and W. Rawicz, Phys. Rev. Lett. **64**, 2094 (1990).
[32] G. Napoli and S. Turzi, Comp. Math. Appl. **55**, 299 (2008).